A Fully Automated Method Using Active Contours for the Evaluation of the Intima-Media Thickness in Carotid US images

Styliani Petroudi, Christos Loizou, Marios Pantziaris, Marios Pattichis and Constantinos Pattichis

Abstract— The thickness of the intima-media complex (IMC) of the common carotid artery (CCA) wall is important in the evaluation of the risk for the development of atherosclerosis. This paper presents a fully automated algorithm for the segmentation of the IMC. The segmentation of the IMC of the CCA wall is important for the evaluation of the intima media thickness (IMT) on B-mode ultrasound images. The presented algorithm is based on active contours and active contours without edges. It begins with image normalization, followed by speckle removal. The level set formulation of Chan and Vese using random initialization provides a segmentation of the CCA ultrasound (US) images into different distinct regions, one of which corresponds to the carotid wall region above the lumen whilst another corresponds to the carotid wall region below the lumen and includes the IMC. The results of the corresponding segmentation combined with anatomical information provide a very accurate outline of the lumen-intima boundary. This outline serves as an excellent initialization for segmentation of the IMC using parametric active contours. The method lends itself to the development of a fully automated method for the delineation of the IMC. The mean and standard deviation of the thickness of the automatically segmented regions are 0.65 mm +/- 0.17 mm and the corresponding values for the ground truth IMT are 0.66 mm +/- 0.18 mm. The Wilcoxon rank sum test shows no significant difference.

I. INTRODUCTION

Cardiovascular Disease (CVD) is one of the most common causes of death in the western world and stroke the most common cause of disability in women. The main pathophysiological mechanism leading to CVD is the development of atherosclerosis: the degeneration of the arterial walls though lipid and other blood-borne material on vascular territories throughout the body. Carotid intima media thickness (IMT) is a measure of early atherosclerosis which can be evaluated non-invasively and with low cost, using high-resolution ultrasound (US). It is the distance between the lumen-intima and the media-adventitia interfaces; and can be seen in US as the double line pattern on both walls of the longitudinal images of the common carotid artery (CCA) [1].

Carotid IMT is correlated with all traditional vascular risk factors and regarded as an intermediate phenotype of atherosclerosis or a marker of subclinical organ damage and

Styliani Petroudi and Constantinos Pattichis are with the Department of Computer Science at the University of Cyprus, P.O. Box 20537 1678 Nicosia, Cyprus. styliani@ucy.ac.cy, pattichi@ucy.ac.cy

C. Loizou is with the Department of Computer Science, Intercollege, Limassol, Cyprus. loizou.c@lim.intercollege.ac.cy

M. Pantziaris is with the Cyprus Institute of Neurology and Genetics, Nicosia, Cyprus. pantziari@cing.ac.cy

Marios Pattichis is with the Department of Electrical and Computer Engineering, The University of New Mexico, Albuquerque, NM 87131 USA. pattichis@ece.unm.edu
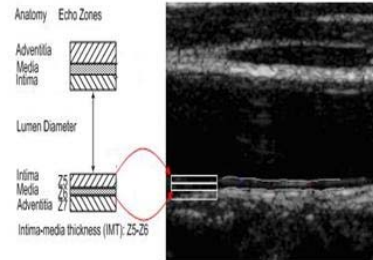
Fig. 1. The intima media complex and measurements thereof. Reproduced from [2].

has been shown to positively correlate with the severity of atherosclerosis and independently predict cardiovascular events [3]. Thus, the IMT may be used for the screening of population as at least half of premature heart attacks and strokes, can, and should, be prevented. IMT can be measured through segmentation of the intima media complex (IMC), which corresponds to the intima and media layers (see Fig. 1) of the arterial wall. Determination of the IMC boundaries is however a complicated task, as the IMC is a thin, relatively low contrast structure, that can be obstructed by ultrasound artifacts, may appear differently due to either different imaging angles and/or differences in anatomy and deteriorates with age [4].

There is a number of techniques that have been proposed for the segmentation of the IMC [5], [6], [7], [8], [9], however most of them are semi-automatic and need user intervention. Pignoli and Longo [5] were the first to tackle the evaluation of the IMT using the intensity outline from the center of the lumen to the corresponding borders. Selzer *et al.* [10] presented a tracking edge method, where the user uses a mouse to identify a few points along the intima and media boundaries. The algorithm fits a smooth curve through these points and uses it as a guide for edge detection, searching in the vicinity of this curve evaluating intensity gradients. Liang *et al.* [6] used dynamic programming incorporating multiple image features at different scales for a fuzzy membership function. In case of ambiguous cases the user can intervene. Cheng *et al.* [8] proposed a method using active contours for the evaluation of the IMT. Their algorithm needs an initialization where the user locates points near the intima-lumen boundary. Stein *et al.* [9] presented a method where after the user identified a position in the lumen the algorithm evaluated the IMT using intensity and gradient information combined with morphological smoothing. Loizou *et al.* [2] presented a semi-automatic method for IMC segmentation

that incorporated the use of active contours in a normalized rectangular region of interest where speckle removal had been applied. A review of the state of the arts algorithms for IMT evaluation is presented in [11]. This work presents a fully automated algorithm for the segmentation of the IMC. The algorithm uses active contours [12], and active contours without edges [13]. Active contours without edges [13] with the incorporation of anatomical information are used to establish intensity information for the US images normalization. Following image normalization active contours without edges are again used to identify an initial intima-media boundary. This boundary provides an excellent, completely automatic initialization for the snake segmentation algorithm that gives the final IMC segmentation. The resulting fully automated segmentation is validated against an expert clinician's manual IMC segmentation and corresponding IMT measures. The following section presents the method in greater detail. Finally the resulting segmentation and corresponding measures are presented and discussed.

II. METHOD

The presented method is based on the use of active contours and active contours without edges to segment different regions in the carotid US images. Active contours [12] face a number of limitations such as initial conditions, curve parameterization and the inability to deal with images where the different structures have many components. The level set formulation of the active contours without edges by Chan and Vese [13] represents curves in an implicit manner, and can handle changes in topology [14], which has been one of the main difficulties snake based CCA algorithms faced [2], [8]. The active contours without edges algorithm [13] is used to segment the US images into the lumen and the carotid wall, and the segmentation results are combined with standard anatomical information to evaluate the needed parameters for accurate segmentation of the IMC at different stages of the algorithm.

A. Characteristics of US Longitudinal CCA Images

For the evaluation of the IMT, B-mode longitudinal US images of the CCA are used, which display the vascular wall as a regular pattern that correlates with anatomical layers. The images cover longitudinally the carotid artery and show the near wall, the lumen and the far wall as shown in Fig. 1. IMT appears as a double-line pattern on both walls of the CCA in the longitudinal US image, and consists of the leading edges of two anatomical boundaries: the lumen-intima and media-adventitia. Anatomical and tissue characteristics and differences result in the lumen appearing as a large longitudinal passage between two brighter regions. The adventitia layer is echogenic and in turn appears as much brighter. The profile of a vertical line, perpendicular to the lumen, near the middle of the CCA US image, shows the anatomical differentiations with corresponding variations in image intensity. The CCA US image's characteristics due to the imaged anatomy provide valuable additional information for fully automating the IMC segmentation and IMT evaluation algorithm.

The presented algorithm explores these anatomical characteristic differences of the CCA, to achieve segmentation of the IMC and evaluation of the IMT.

B. Speckle Removal

Speckle is a form of granular multiplicative noise caused when the surface imaged appears rough to the scale of the wavelength used. The edges of the adventitia are also affected by this noise. Thus, prior to any other filtering, the speckle removal linear scaling filter that utilizes local mean and variance, as in [15], is applied to despeckle the image.

C. Segmentation Using Active Contours Without Edges and Image Normalization

A fully automated IMC segmentation algorithm needs to be able to work on all images despite variability due to capture time, settings and scanners. Normalization of B-mode US images for the CCA has been shown to address this variability using intensity adjustments that take into account anatomy and differences in tissue attenuation. The normalization method proposed in [15] performs linear grayscale remapping so that median intensity value of the artery lumen has intensities between 0 and 5, and the median intensity value of the adventitia between 180 and 190 for 8 bit US images [16]. The normalization reduces image variability due to the reasons aforementioned. However, the normalization in [15] requires human interaction for choosing a region in the lumen and another in the adventitia so that corresponding intensity values are established for the intensity remapping. Automatation of the image normalization can be achieved with the use of the level set formulation of the active contours without edges [13].

Level set methods [14] offer a highly robust and accurate method for tracking interfaces moving under complex motions: they work in a number of space dimensions but more importantly they can handle topological changes naturally. The level set image segmentation is based on the idea of embedding a closed curve Γ in $\mathbb{R}^2$ into a surface in $\mathbb{R}^3$. Embedding is achieved through the definition of a suitable function $\phi : \mathbb{R}^3 \times \mathbb{R}^+ \to \mathbb{R}$, known as the level set function. The level set method takes the perspective of viewing Γ as the zero level set of a function ϕ from $\mathbb{R}^2$ to $\mathbb{R}$, [14]. Using the level set formulation of the active contours without edges by Chan and Vese [13] - from now onwards referred to as the Chan-Vese model-, the regions corresponding to the lumen and the carotid wall (including the intima, the media and the adventitia) can be automatically segmented.

The Chan-Vese model [13] corresponds to a region-based level set method which uses the Mumford-Shah functional in the level set framework for a piecewise constant representation of an image. Evolution of the curve is governed by properties of the region of the image $u_0(x,y)$ enclosed by the curve. The model tries to separate the image into regions based on pixel intensities and introduces the following energy

functional:

$$F(c_1, c_2, C) = \mu \ . \ Lenght(C) + \nu \ . \ Area(inside(C))$$

$$+ \lambda_1 \int_{inside(C)} |u_0(x,y) - c_1|^2 dxdy$$

$$+ \lambda_2 \int_{outside(C)} |u_0(x,y) - c_2|^2 dxdy \quad (1)$$

where $\mu \geq 0$, $\nu \geq 0$, λ_1, $\lambda_2 > 0$, are fixed parameters. Eq. (1) is a generalization of the Mumford-Shah functional as introduced in [17]. Segmentation becomes the minimization problem of:

$$\inf_{c_1, c_2, C} F(c_1, c_2, C) \quad (2)$$

μ corresponds to the perimeter length regularization parameter and ν corresponds to the area regularization parameter. c_1 is the mean of u_0 inside the curve C, and c_2 is the mean of u_0 outside the curve C. In almost all numerical calculations, including this implementation $\lambda_1 = \lambda_2 = 1$ and $\nu = 0$. This minimal partition problem is formulated and solved using level sets [13]. For evaluation of the level sets in addition to the value of the parameters set above, $\mu = 0.2$ and h the space step is set to 1 whilst, Δt, the time step, is set to 0.5. The initialization contour is a randomly placed disc with radius 0.9 mm.

After the Chan-Vese model is applied the image is segmented into a number of regions some corresponding to the artery wall whilst others to the background and the lumen. More importantly, the resulting segmentation can also serve as an excellent initialization for the active contours for segmentation of the IMC. Without loss of generality, for establishing the adventitia and the lumen, the areas corresponding to the first centile in the left and the last centile in the right are set to zero intensity, as are the first centile on the top and the last on the bottom. The region of interest is thus restricted. Following, only the regions with an area larger than 18 mm^2 are considered. By running a line vertically across the middle of the US image, the largest region on the bottom correspond to the far carotid wall, whilst the background region above it corresponds to the lumen. By evaluating the intensities in the corresponding regions, the values for image normalization can be obtained.

Figure 2 shows the initialization of the Chan-Vese segmentation and results of the Chan-Vese algorithm. It can be seen that the largest region in the bottom of Figure 2c corresponds to the far wall three layers (intima-media-adventitia) of the CCA. The segmentation of this region provides the required intensity information to achieve image normalization. More importantly the boundary of this region provides the outline for initialization of the parametric active contour segmentation, as described in the following section.

D. Segmentation of the IMC using Active Contours

Following speckle removal and image normalization, the Chan-Vese algorithm [13] is applied again in the same way as in the previous sub-section, and the far wall adventitia is established. A closing operation with a 0.18 mm radius disc smooths the outline of the segmented region and the boundary between the adventitia and the lumen is extracted. This boundary provides an excellent initialization for segmentation of the IMC using snakes [12], as in [2]. The boundary which approximates very closely the lumen-intima boundary, provides the contour points needed. Twenty contour points are chosen, equally spaced along the identified interface, and are matched with twenty points which are displaced 0.9 mm downwards in the vertical direction. This displacement is based on the observation that the IMT lies between 0.6 and 1.4 mm, with a mean IMT of 1.0 mm [18]. Unlike [2], the initialization points are equally spaced. Segmentation of the IMC is achieved by minimizing the energy functional of the active contours extension by Williams and Shah [19]:

$$E_{snake}^* = \int_0^1 E_{snake}(\mathbf{v}(s))ds$$

$$= \int_0^1 E_{internal}(\mathbf{v}(s)) + E_{image}(\mathbf{v}(s)) + E_{constraints}(\mathbf{v}(s)) \ ds$$
(3)

where $\mathbf{v}(s) = (x(s), y(s))$ is the vector representation of the contour with the arc length s as the parameter. The parameters α, β and γ are used to balance the relative influence of the three energy term, the two internal energy terms that impose continuity constraints and the external image energy term that incorporates local gradient magnitude. For initialization of the snake deformation and the minimization of Eq. (3) the following initial values are used: $\alpha_i(s) = 0.6$, $\beta_i(s) = 0.4$ and $\gamma_i(s) = 2$, as in [8] and [2]. The resulting segmentation corresponds to the IMC.

III. RESULTS

The algorithm is evaluated on longitudinal US images of the CCA obtained from 30 normal asymptomatic subjects acquired by the ATL HDI-3000 ultrasound scanner (Advanced Technology Laboratories, Seattle, USA), with a 4-7 MHz 38 mm linear array transducer. The 8-bit images (i.e. with intensity ranging from 0 to 255) were resized using the bi-cubic method to have resolution of 16.66 pixels/mm (i.e. the spatial resolution is 0.06 mm) and a corresponding size of 768×576 pixels in order to maintain uniformity in the digital image spatial resolution [2]. An expert vascular clinician delineated the IMT on the US images by defining about 20 consecutive points on the IMT border. For the delineations if should be noted that the lumen-intima frontiers are more visible in the far wall, and thus the corresponding regions are used for ground truth evaluation. Figures 3 and 4 show the results of the segmentation of the IMC using the presented method and compare the results to the ground truth segmentations. By observing the difference between the two segmentations one can see how closely the algorithm approximates the clinician's evaluation.

The results of the algorithm are quantitatively evaluated and compared to the ground truth provided by the clinician using different measures. The measures evaluated are the area overlap accuracy, the mean IMT value and IMT difference. Table I presents analytically the difference between the IMT
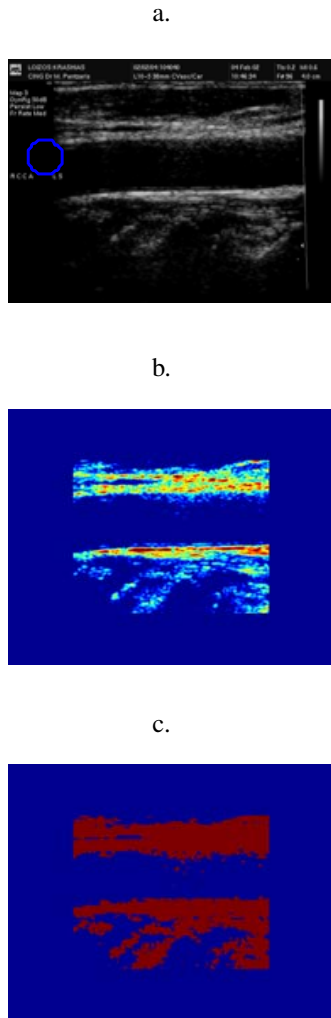
a.

b.

c.

Fig. 2. The level set segmentation of CCA image. a) Level set initialization, b) Segmentation of the US image in different regions, c) The segmented regions intima-media-adventitia.
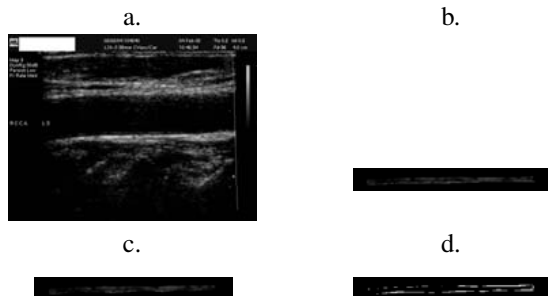

Fig. 3. Example of presented segmentation of the IMC for the CCA shown in Figure 2. a) The original CCA US image, b) the expert's ground truth segmentation, c) the automated segmentation that results from the application of the presented algorithm, d) the difference between the ground truth segmentation and the automated segmentation.
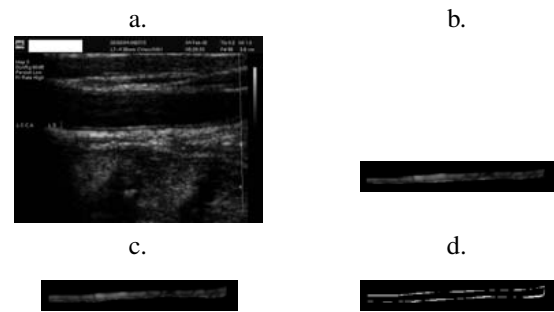

Fig. 4. Another example of the application of the presented IMC segmentation algorithm: a) The original CCA US image, b) the expert's ground truth segmentation, c) the automated segmentation that results from the application of the presented algorithm, d) the difference between the ground truth segmentation and the automated segmentation.

TABLE I

ANALYTICAL EVALUATION OF THE PRESENTED METHOD SHOWING THE
FIVE BEST AND WORST CASES, AS WELL AS COMPARISON STATISTICS
FOR THE ENTIRE DATABASE

	Evaluated IMT in mm	Ground Truth IMT in mm	Percentage Error
Case_best 1	0.72	0.72	0.59
Case_best 2	0.52	0.51	2.03
Case_best 3	0.55	0.54	1.93
Case_best 4	0.49	0.48	3.42
Case_best 5	0.71	0.69	2.54
Case_worst 1	0.95	0.51	87.40
Case_worst 2	0.91	1.16	20.90
Case_worst 3	0.49	0.63	21.80
Case_worst 4	0.53	0.65	18.93
Case_worst 5	0.53	0.65	18.12
Mean	0.65	0.66	
Std Deviation	0.17	0.18	

evaluation using the presented method versus the expert's evaluation and compares the first and second order statistics for the IMT value measurements and ground truth for all 30 cases. The percentage difference versus the ground truth is also provided for the individual cases in percentages. The mean value of the absolute IMT difference is 0.09 mm with the minimum difference at 0.004 mm and the maximum difference at 0.44 mm, with a standard deviation of 0.10 as shown in Table II, whilst the difference between the evaluated and ground truth IMT mean values is in the range of 0.01 mm. The algorithm compares favorably to other automated methods in the literature which achieve errors over 1 mm [11]. The mean value of the IMT resulting from the automatic segmentation using the presented algorithm is 0.65+/-0.17 mm and the corresponding value for the ground truth IMT is 0.66+/-0.18 mm. At the images' given resolution the mean difference corresponds to a mean difference of a pixel. The Wilcoxon rank sum test confirms with a p-value of 0.89 at the 5% significance level that there are no significant differences between the IMT measurements based on the ground truth and the automatic segmentation.

TABLE II
FURTHER QUANTITATIVE EVALUATION OF THE PRESENTED METHOD VS
THE EXPERT'S SEGMENTATION

	Mean	Standard Deviation
Accuracy of area overlap (in %)	91.1	4.2
IMT difference (in mm)	0.09	0.10

IV. DISCUSSION

The proposed method for IMC segmentation and evaluation of the IMT is completely automated and robust. The results show very good agreement with the expert clinician's segmentation, though an evaluation on a larger dataset will take place. The good agreement with the expert's evaluations of the IMC and the IMT are due to the use of the level set formulation of the Chan-Vese method with the incorporation of anatomical information for the parametric contour initialization as the image is composed and thus segmented in two main regions, the lumen and the carotid wall. Additionally, the Chan-Vese model is not based on an edge function, thus there is no need in smoothing the initial image, the model works well with noisy images, the level set formulation allows for easy incorporation of topological changes and the initial contour has not influence on the resulting segmentation.

The method is completely automated, fast and does not require any user interaction. The evaluation of the method results in a mean of IMT difference of 0.09 mm with a standard deviation of 0.10 mm and compares favorably to other automated methods presented in the literature reaching at best a mean difference of 0.10 mm [11].

V. CONCLUSIONS AND FUTURE WORK

This paper presents a fully automated method for the segmentation of the IMC so that the IMT can be evaluated. The IMC in the near wall of the CCA is not properly imaged due to the nature of US imaging, thus the segmentation algorithm is developed for segmentation of the IMC at the far wall, where the borders are visible [5]. The success of the algorithm is due to the use of the available anatomical information regarding the position and general structure of the CCA to establish the best possible outcome. The Chan-Vese model [13] achieves very good segmentation results as it inherently separates the image in two distinct regions the CCA wall and the lumen.

The algorithm is evaluated on images from 30 cases with a mean IMT difference of 0.09 mm. The algorithm works well even on difficult cases, but further evaluation is required. Future work will involve assessment of the algorithm on a much larger dataset and discussion of how inter- and intra-observer variability affects the evaluation of the results.

VI. ACKNOWLEDGMENTS

REFERENCES

[1] P. Touboul, M. Hennerici, S. Meairs, H. Adams, P. Amarenco, N. Bornstein, L. Csiba, M. Desvarieux, S. Ebrahim, and et al., "Mannheim carotid intima-media thickness consensus (2004–2006)," *Cerebrovascular Diseases*, vol. 23, pp. 75–80, 2007.

[2] C. Loizou, C. Pattichis, M. Pantziaris, T. Tyllis, and A. Nicolaides, "Snakes based segmentation of the common carotid artery intima media," *Medical and Biological Engineering and Computing*, vol. 45, pp. 35–49, 2007.

[3] M. W. Lorenz, H. S. Markus, M. L. Bots, M. Rosvall, and M. Sitzer, "Prediction of clinical cardiovascular events with carotid intima-media thickness: A systematic review and meta-analysis," *Circulation*, vol. 115, no. 4, pp. 459–467, 2007.

[4] D. Lamont, L. Parker, M. White, N. Unwin, S. M. A. Bennett, M. Cohen, D. Richardson, H. O. Dickinson, A. Adamson, K. G. M. Alberti, and A. W. Craft, "Risk of cardiovascular disease measured by carotid intima-media thickness at age 49-51: lifecourse study," *British Medical Journal*, vol. 320, no. 7230, pp. 273–278, 2000.

[5] P. Pignoli and T. Longo, "Evaluation of atherosclerosis with b-mode ultrasound imaging," *Journal of Nuclear Medicine and Allied Sciences*, vol. 32, pp. 166–173, 1988.

[6] Q. Liang, I. Wendelhag, J. Wikstrand, and T. Gustavsson, "A multiscale dynamic programming procedure for boundary detection in ultrasonic artery images," *Medical Imaging, IEEE Transactions on*, vol. 19, no. 2, pp. 127 –142, 2000.

[7] R. H. Selzer, W. J. Mack, P. L. Lee, H. Kwong-Fu, and H. N. Hodis, "Improved common carotid elasticity and intima-media thickness measurements from computer analysis of sequential ultrasound frames," *Atherosclerosis*, vol. 154, no. 1, pp. 185 – 193, 2001.

[8] D. Cheng, A. Schmidt, K. Cheng, and H. Burkhardt, "Using snakes to detect the intimal and adventitial layers of the common carotid artery wall in sonographic images," *Computer Methods and Programs in Biomedicine*, vol. 67, no. 1, pp. 27 – 37, 2002.

[9] J. H. Stein, C. E. Korcarz, M. E. Mays, P. S. Douglas, M. Palta, H. Zhang, T. LeCaire, D. Paine, D. Gustafson, and L. Fan, "A semiautomated ultrasound border detection program that facilitates clinical measurement of ultrasound carotid intima-media thickness," *Journal of the American Society of Echocardiography*, vol. 18, no. 3, pp. 244 – 251, 2005.

[10] R. H. Selzer, H. N. Hodis, H. Kwong-Fu, W. J. Mack, P. L. Lee, C. ran Liu, and C. hua Liu, "Evaluation of computerized edge tracking for quantifying intima-media thickness of the common carotid artery from b-mode ultrasound images," *Atherosclerosis*, vol. 111, no. 1, pp. 1 – 11, 1994.

[11] F. Molinari, G. Zeng, and J. S. Suri, "A state of the art review on intima-media thickness (imt) measurement and wall segmentation techniques for carotid ultrasound," *Computer Methods and Programs in Biomedicine*, vol. 100, pp. 201 – 221, 2010.

[12] M. Kass, A. Witkin, and D. Terzopoulos, "Snakes: Active contour models," *International Journal of Computer Vision*, vol. 1, pp. 321–331, 1988.

[13] T. Chan and L. Vese, "Active contours without edges," *IEEE Transactions on Image Processing*, vol. 10, pp. 266 –277, 2001.

[14] S. Osher and J. A. Sethian, "Fronts propagating with curvature-dependent speed: algorithms based on hamilton-jacobi formulations," *Journal of Computational Physics*, vol. 79, pp. 12–49, 1988.

[15] C. Loizou, C. Pattichis, M. Pantziaris, T. Tyllis, and A. Nicolaides, "Quality evaluation of ultrasound imaging in the carotid artery based on normalization and speckle reduction filtering," *Medical and Biological Engineering and Computing*, vol. 44, pp. 414–426, 2006.

[16] T. J. Tegos, M. M. Sabetai, A. N. Nicolaides, T. S. Elatrozy, S. Dhanjil, and J. M. Stevens, "Patterns of brain computed tomography infarction and carotid plaque echogenicity," *Journal of Vascular Surgery*, vol. 33, no. 2, pp. 334 – 339, 2001.

[17] D. Mumford and J. Shah, "Optimal approximation by piecewise smooth functions and associaated variational problems," *Communication of Pure and Applied Mathematics*, vol. 42, pp. 577–685, 1989.

[18] I. Wendelhag, Q. Liang, T. Gustavsson, and J. Wikstrand, "A new automated computerized analyzing system simplifies readings and reduces the variability in ultrasound measurement of intima-media thickness," *Stroke*, vol. 28, no. 11, pp. 2195–2200, 1997.

[19] D. J. Williams and M. Shah, "A fast algorithm for active contours and curvature estimation," *International Journal on Graphics, Vision and Image Processing: Image Understanding*, vol. 55, pp. 14 – 26, 1992.